

Electronic Supplementary Information

for

Bromine atom introduction improves F⁻ sensing ability of indolo[3, 2-b]carbazole-salicylaldehyde-based fluorescence turn-on sensor

Lihua Xu, Jiang Zhao*

School of Chemistry and Chemical Engineering, Guizhou University, Guiyang 550025,

P. R. China.

*Corresponding Author E-mail: jiangzhao@gzu.edu.cn. (J. Zhao)

Information for the Experimental Section

Reagents and Materials

Commercial reagents DMF, DMSO, THF, CH₃CN, anhydrous ethanol, methanol, 1, 4-dioxane, dichloromethane, petroleum ether, glacial acetic acid, concentrated sulfuric acid were all analytical grades. The experimental water was secondary deionized water. For the synthesis of **ICZ-p1-S** and **Br-ICZ-p1-S**, the tetrakis(triphenylphosphine)palladium were prepared from literatures^[1], the starting materials of the Pd(dppf)Cl₂, 1, 4-cyclohexanedione, phenylhydrazine hydrochloride, 4-bromophenylhydrazine hydrochloride, 1-bromobutane, n-bromosuccinimide (NBS), 5-bromo-2-hydroxybenzaldehyde, bis (pinacolato) diboron, tert-butyl dimethylchlorosilane, potassium hydroxide, sodium acetate, sodium carbonate, imidazole, tetrabutylammonium salt (F⁻, Cl⁻, Br⁻, I⁻, AcO⁻, BF₄⁻, PF₆⁻, HSO₄⁻, NO₃⁻, CN⁻, ClO₄⁻ and H₂PO₄⁻) were purchased from a commercial supplier (Shanghai Energy & Chemical, China) and can be used without further purification.

Physical Characterization

¹H-NMR, ¹³C-NMR spectra were measured in DMSO and CDCl₃ with a JNM-ECZ400s MHz spectrometer with the chemical shifts quoted relative to tetramethylsilane (TMS) at room temperature. High resolution TOF-MS data were recorded at the Agilent 6545 Q-TOF LC/MS. **ICZ-p1-S** crystal was obtained by slow evaporation at room temperature after acetonitrile dissolution, and then its single crystal X-ray data were collected on Bruker D8 VENTURE. The UV-Vis spectra and the fluorescent spectra were obtained by UV-2700 double beam UV-visible

spectrophotometer and Varian Cary Eclipse fluorescence spectrometer. The excitation wavelength measured by solution PL was set to 332 nm. The relevant data of time dependent density functional theory (TD-DFT) calculation was collected by using the Gaussian 16 software with B3LYP/6-311g* basis set.

Anion sensing studies

The probes **ICZ-p1-S** and **Br-ICZ-p1-S** were dissolved in acetonitrile to produce a 2×10^{-3} M solution, and were diluted 100 times to obtain the final test concentration of 2.0×10^{-5} M. The tetrabutylammonium salt solution of each anion was prepared in acetonitrile to 2.0×10^{-2} M. The anion solution was added into the probe solution, and the spectral data were recorded by UV-vis and emission spectra to investigate the selectivity of the probe to anions (F^- , Cl^- , Br^- , I^- , AcO^- , BF_4^- , PF_6^- , HSO_4^- , NO_3^- , CN^- , ClO_4^- and $H_2PO_4^-$).

Limit of detection (LOD)

The LOD of the fluoride ion were calculated according to the following formula:

$$LOD = 3\delta/c/k$$

δ : Standard deviation, which was obtained by measuring the fluorescence intensity of **ICZ-p1-S** and **Br-ICZ-p1-S** in CH_3CN (blank solution) over 20 times and calculating according to the standard deviation formula, the related spectra and data are shown in **Fig S5**; k : Add different times of fluoride ion solution into the same probe solution in sequence, and record the related fluorescence intensity of the sensor- F^- solutions,

thereby the fluorescence intensities corresponding to different multiples of fluoride ions were plotted, and then the slope was obtained by linear fitting; C: Molar concentration of probes solution.

Job's plot experiment

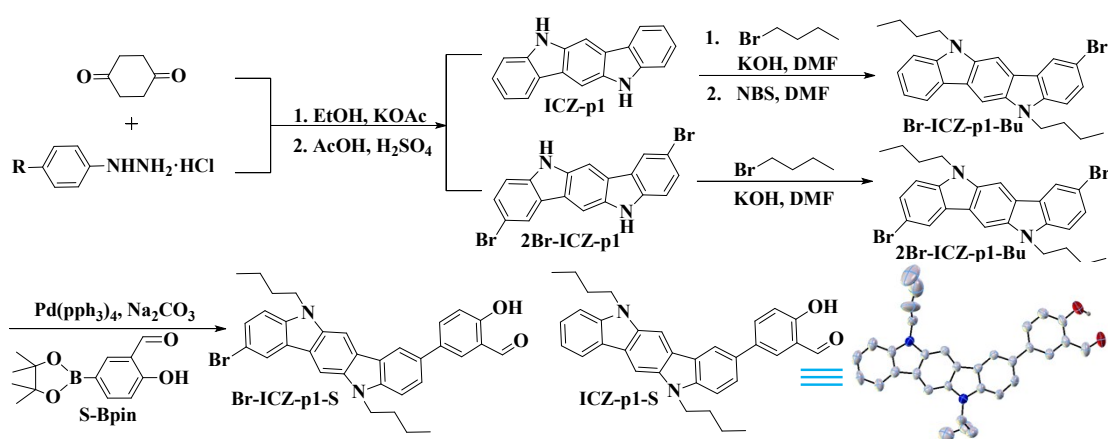
Keeping the volume and total concentration of a testing solution at 3 mL and 4.0×10^{-6} M, and the concentration ratio between the sensor and sensor- F^- is set as 0.0, 0.1, 0.2, 0.3, 0.4, 0.5, 0.6, 0.7, 0.8, 0.9 and 1.0 in such testing solution. Then the fluorescence spectra of the such testing solution were measured at room temperature. Finally, the relationship between the intensity changes of relevant emission maximum and the concentration ratio of F^- to the overall concentration were obtained, namely, the Job's plot.

Spiked recovery experiments

Firstly, 3 mL of the sensor solution (2×10^{-5} M) was added to the cuvette, by adding equal amounts of fluoride ion pure water solutions (2×10^{-2} M, 0.5 equiv.) in sequence into the sensor solutions (2×10^{-5} M), until the fluorescence intensities were no longer changed, the fluorescence titration spectra were obtained (**Fig S7**). Then linear fitting plots were drawn for different fluoride ion concentrations and fluorescence intensity of the sensor- F^- mixtures (**Fig S8**). For the Yuehu Lake water and tap water real samples, the concentrations of spiked fluoride ions were 1, 3, and 5×10^{-5} mol/L (C_{taken}), the fluorescence intensity of these fluoride ion spiked real samples and sensors mixtures were measured (**Fig S9**), 3 times of parallel experiments for each spiked real sample were conducted, and the average values of the concentrations can be obtained, which

defined as the C_{found} in **Table S2**. The actual concentration of spiked fluoride ion concentration was calculated through the formula in the calibration curve diagram (**Table S3**). According to the following formula, the average recovery rate (R%) and relative error (RE%), as well as the relative standard deviation (RSD%), can be calculated.

Synthesis



Scheme S1. Synthetic routes for **ICZ-p1-S** and **Br-ICZ-p1-S**, and the ORTEP crystal structures of the **ICZ-p1-S**, CCDC NO.: 2312194.

For the synthesis scheme of indolocarbazole (ICZ), the compounds were named **ICZ-p1-S** and **Br-ICZ-p1-S** according to the presence or absence of halogen atomic bromine. The general procedures for synthesizing **ICZ-p1-S** and **Br-ICZ-p1-S** are as follows. The synthesis methods of **ICZ-p1**, **2Br-ICZ-p1**, **2Br-ICZ-p1-Bu** and **S-Bpin** have been reported^[2-4].

ICZ-p1-Bu:

The **ICZ-p1** (1.0 equiv.) and KOH (2.5 equiv.) were dissolved in DMF. The mixture was stirred for half an hour at room temperature. Then, 1-bromobutane (2.5 equiv.) was dropped into the reaction flask at 0 °C and heated to 25 °C for 10 hours. The mixture was dried and purified with dichloromethane/petroleum ether (1:2) as eluent by column

chromatography. **ICZ-p1-Bu** as yellow solid, yield (75.36%). ¹H NMR (400 MHz, CDCl₃) δ 8.21 (d, *J* = 7.7 Hz, 2H), 8.02 (s, 2H), 7.51 – 7.46 (m, 2H), 7.42 (d, *J* = 8.1 Hz, 2H), 7.25 – 7.20 (m, 2H), 4.42 (t, *J* = 7.2 Hz, 4H), 1.99 – 1.91 (m, 4H), 1.48 (dd, *J* = 15.2, 7.5 Hz, 4H), 0.98 (t, *J* = 7.4 Hz, 6H).

Br-ICZ-p1-Bu:

The **ICZ-p1-Bu** (1.0 equiv.) was dissolved in THF solution and cooled with an ice bath. N-bromosuccinimide (NBS) was added in small amounts (1.1 equiv.) in several batches under light-shielding condition. The temperature was increased to room temperature gradually and held for 4 hours. The **1Br-ICZ-p1-Bu** as yellow-green solid was purified by column chromatography using dichloromethane/petroleum ether (1:15) as eluent (yield 57.67%). ¹H NMR (400 MHz, CDCl₃) δ 8.31 (d, *J* = 1.9 Hz, 1H), 8.20 (d, *J* = 7.7 Hz, 1H), 8.00 (s, 1H), 7.96 (d, *J* = 0.5 Hz, 1H), 7.54 (dd, *J* = 5.6, 3.0 Hz, 1H), 7.50 (ddd, *J* = 8.2, 7.1, 1.2 Hz, 1H), 7.42 (d, *J* = 8.1 Hz, 1H), 7.28 (d, *J* = 8.6 Hz, 1H), 7.25 – 7.21 (m, 1H), 4.43 – 4.35 (m, 4H), 1.98 – 1.88 (m, 4H), 1.51 – 1.41 (m, 4H), 0.98 (td, *J* = 7.3, 5.4 Hz, 6H).

Synthetic procedures for the sensors: Under a N₂ atmosphere, in a Schlenk tube, the compound **1Br-ICZ-p1** or **2Br-ICZ-p1** (1.0 equiv.) was reacted with the **S-Bpin** (1.2 or 0.9 equiv.) in the presence of the Pd(pph₃)₄ (0.05 equiv.) and 2 M Na₂CO₃ solution (1 equiv.) in THF. Then, the mixture was heated and refluxed for 2 hours. By using dichloromethane : petroleum ether (2 : 3) as eluent, the products were purified via flash column chromatography.

ICZ-p1-S was obtained as yellow solid, yield (51.57%). ¹H NMR (400 MHz, CDCl₃) δ 10.99 (s, 1H), 10.05 (s, 1H), 8.37 (d, *J* = 1.7 Hz, 1H), 8.22 (d, *J* = 7.7 Hz, 1H), 8.05 (d, *J* = 8.7 Hz, 2H), 7.94 (dd, *J* = 8.5, 2.3 Hz, 1H), 7.90 (d, *J* = 2.3 Hz, 1H), 7.66 (dd, *J*

= 8.3, 1.7 Hz, 1H), 7.47 (dt, $J = 16.8, 7.7$ Hz, 3H), 7.23 (d, $J = 7.5$ Hz, 1H), 7.13 (d, $J = 8.5$ Hz, 1H), 4.44 (dd, $J = 14.1, 7.1$ Hz, 4H), 1.96 (dt, $J = 14.2, 7.2$ Hz, 4H), 1.48 (tt, $J = 8.9, 4.4$ Hz, 4H), 0.99 (td, $J = 7.4, 4.8$ Hz, 6H). ^{13}C NMR (101 MHz, CDCl_3) δ 196.98, 160.37, 141.84, 141.19, 136.52, 136.17, 134.67, 131.85, 129.56, 125.92, 124.57, 123.54, 123.21, 122.76, 120.92, 120.34, 118.18, 108.85, 108.54, 99.13, 98.87, 43.26, 31.16, 20.83, 14.11. TOF-MS (ESI): m/z calculated for $\text{C}_{33}\text{H}_{32}\text{N}_2\text{O}_2$: 488.2459[M]⁺, observed :511.2356[M + Na]⁺.

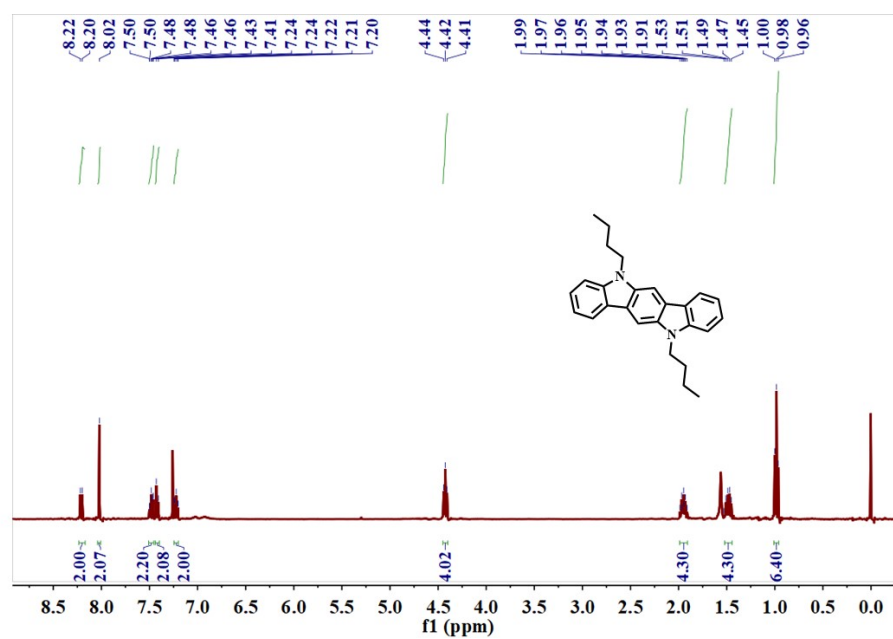
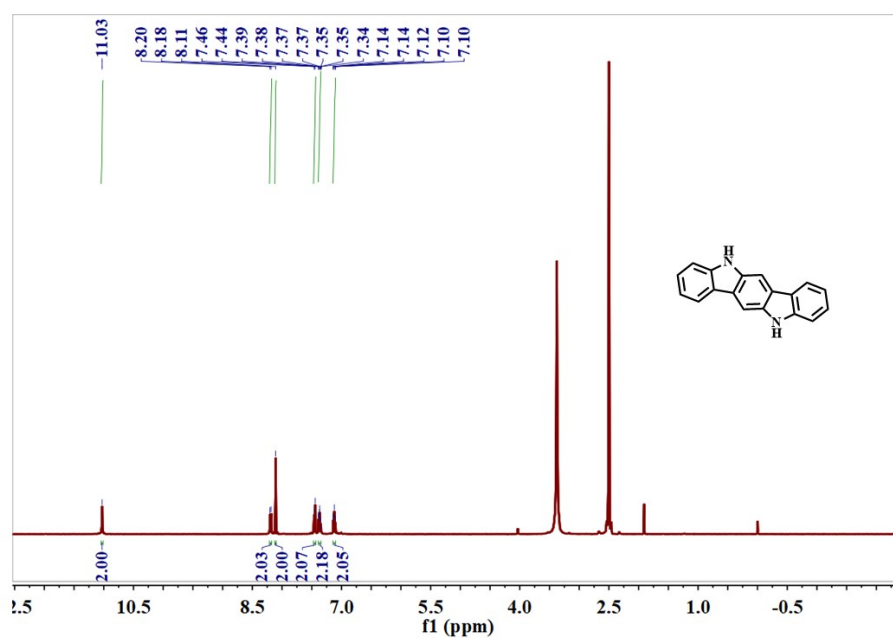
Br-ICZ-p1-S was obtained as light yellowish green solid, yield (32.06%). ^1H NMR (400 MHz, CDCl_3) δ 11.00 (s, 1H), 10.04 (s, 1H), 8.34 (dd, $J = 13.6, 1.8$ Hz, 2H), 8.04 (s, 1H), 7.96 (s, 1H), 7.93 (dd, $J = 8.5, 2.2$ Hz, 1H), 7.89 (d, $J = 2.3$ Hz, 1H), 7.76 – 7.65 (m, 1H), 7.55 (dd, $J = 8.6, 1.8$ Hz, 1H), 7.49 – 7.41 (m, 1H), 7.28 (d, $J = 8.6$ Hz, 1H), 7.13 (d, $J = 8.6$ Hz, 1H), 4.38 (dq, $J = 15.1, 7.5$ Hz, 4H), 1.93 (ddd, $J = 14.9, 11.3, 7.4$ Hz, 4H), 1.45 (ddd, $J = 20.3, 11.2, 6.3$ Hz, 4H), 0.97 (ddd, $J = 10.8, 7.4, 3.2$ Hz, 6H). ^{13}C NMR (101 MHz, CDCl_3) δ 196.95, 160.41, 141.32, 140.38, 136.62, 136.37, 136.12, 134.56, 131.86, 129.74, 128.38, 124.93, 124.57, 123.18, 122.01, 120.91, 118.39, 118.12, 110.72, 109.92, 108.94, 99.18, 43.34, 31.09, 20.80, 14.07. TOF-MS(ESI): m/z calculated for $\text{C}_{33}\text{H}_{31}\text{N}_2\text{O}_2\text{Br}$: 567.1563[M]⁺, observed: 568.1562 [M + H]⁺.

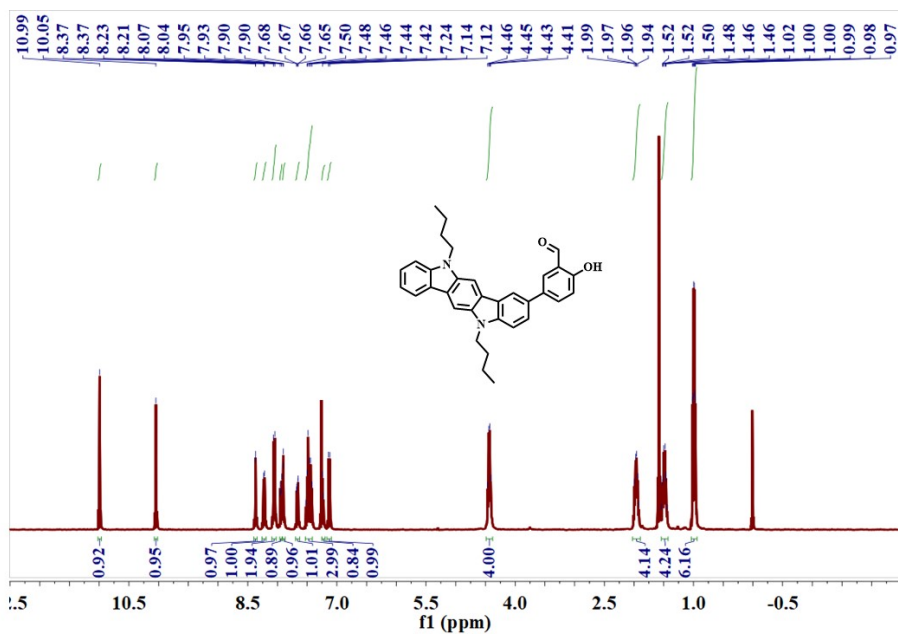
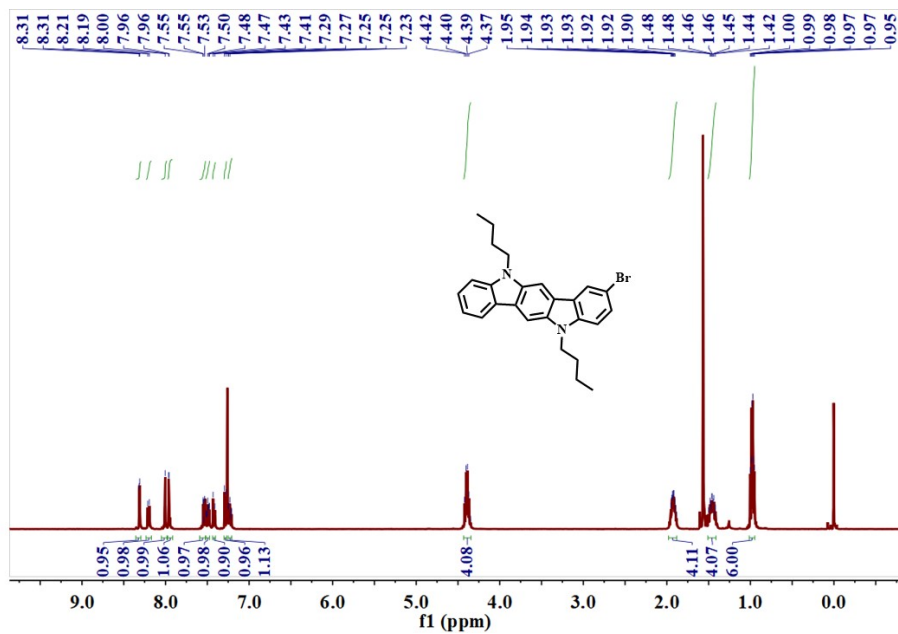
Text S1 for the synthesis discussion of these two sensors

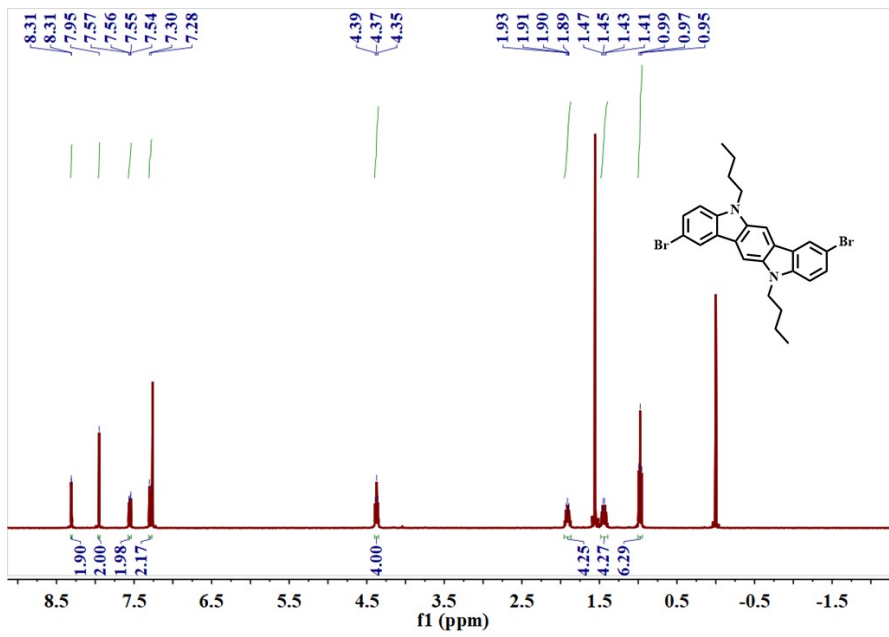
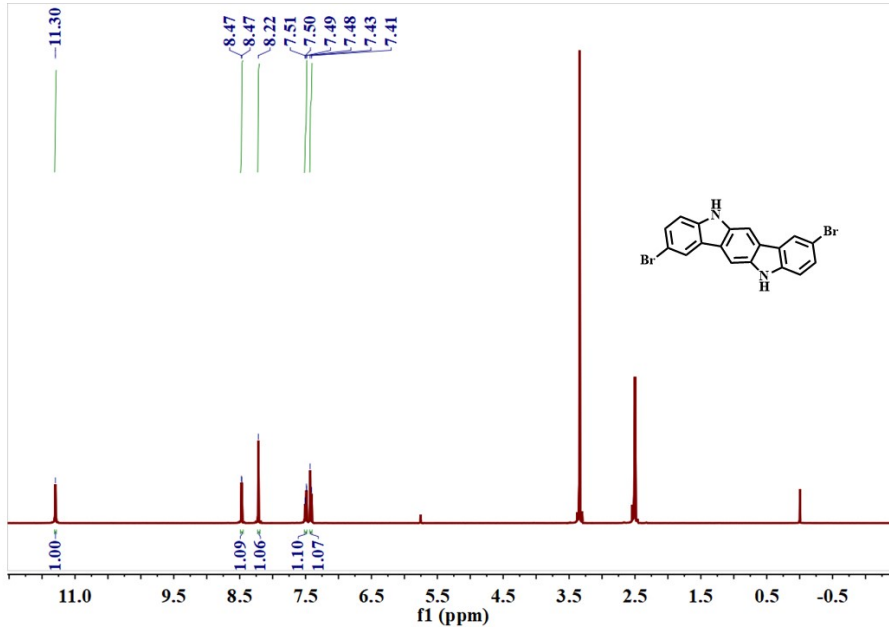
Following the synthetic routes provided in **Scheme S1**, the **ICZ-p1-S** and **Br-ICZ-p1-S** were obtained by Suzuki cross coupling reaction of indolo[3, 2-b]bromide

and salicylaldehyde borate catalyzed by palladium tetrakis (triphenylphosphine). Their chemical structures were confirmed by the ^1H NMR, ^{13}C NMR, TOF-MS spectroscopies and X-ray single crystal diffraction. In their ^1H NMR spectra, the single peaks with chemical shifts of about 11.00 ppm and 10.00 ppm should be derived from the $-\text{OH}$ and $-\text{CHO}$ protons, respectively. The rest of proton peaks with chemical shifts of 6.00 to 9.00 ppm should be attributed to the proton on the aromatic ring of the ICZ backbone and salicylaldehyde unit. The proton signals located at *ca.* 4.40, 1.90, 1.40 and 0.97 ppm were attributed to the methylene and methyl protons on the butane group, respectively (**Fig. S1**). The ^{13}C NMR spectra showed that the chemical shifts around 196.90 ppm should be the carbon signal of carbonyl group. The chemical shifts at about 43.30, 31.10, 20.80, 14.10 ppm should be the carbon signal of butane unit. While, the other chemical shifts should be from the carbon signal of aromatic ring (**Fig. S2**). These results were consistent with the chemical structure characteristics of these sensors, preliminarily indicating the successful synthesis of them. Meanwhile, their TOF-MS data were also acquired, showing the main fragment peaks at m/z 511.2356 and 568.1562, which were consistent with the theoretical values of $[\text{ICZ-p1-S} + \text{Na}]^+$ and $[\text{Br-ICZ-p1-S} + \text{H}]^+$ (**Fig. S3**). It provided further support for the confirmation of their chemical structures. In order to obtain the absolute structure information of these two sensors, **ICZ-p1-S** single crystal was obtained by slowly evaporation in acetonitrile solution. The X-ray single crystal diffraction results were consistent with the molecular structure of the sensor, which more accurately confirmed the successful synthesis of

these sensors (Scheme S1).







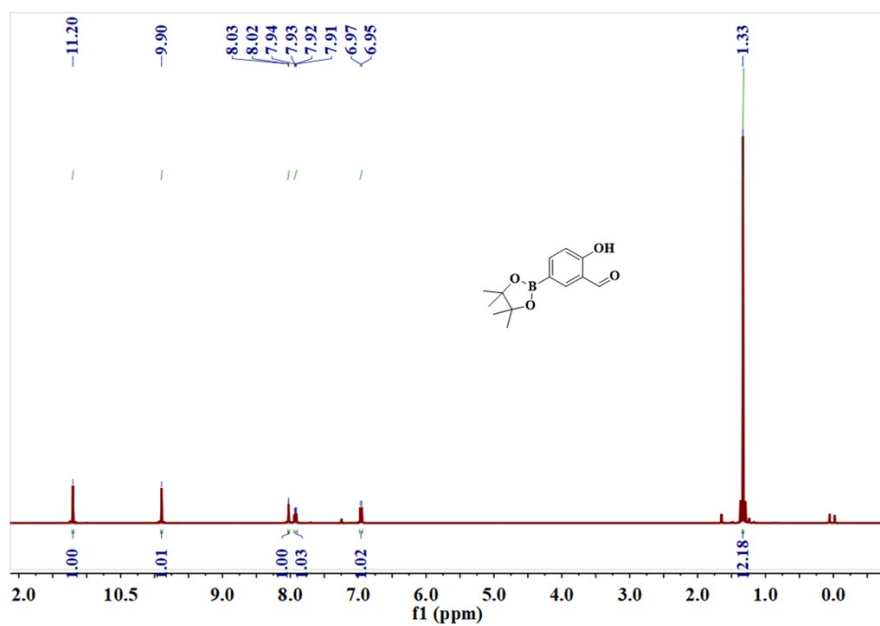
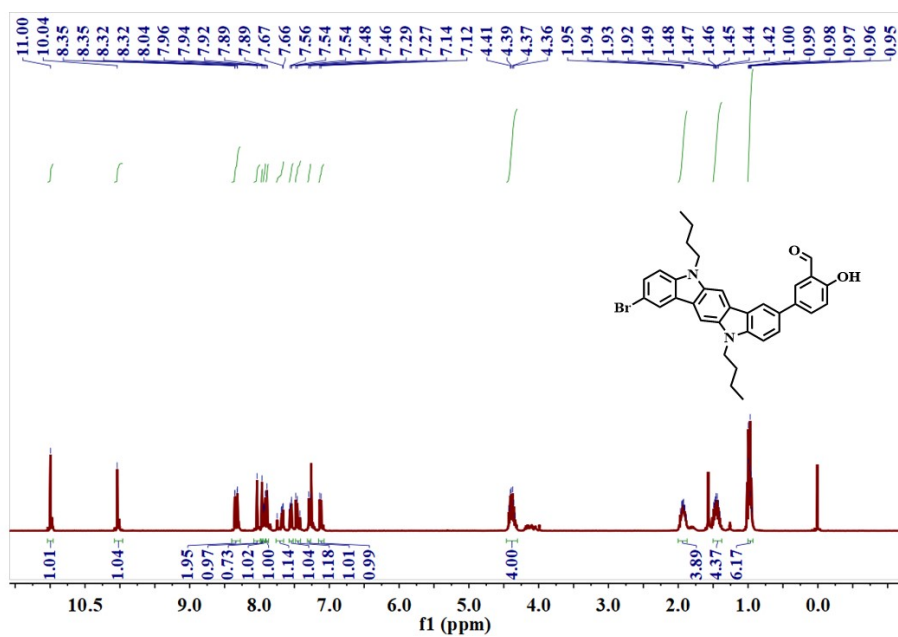


Fig. S1 ^1H NMR spectra of the concerned compounds, and the target compound **ICZ-p1-S** and **Br-ICZ-p1-S**

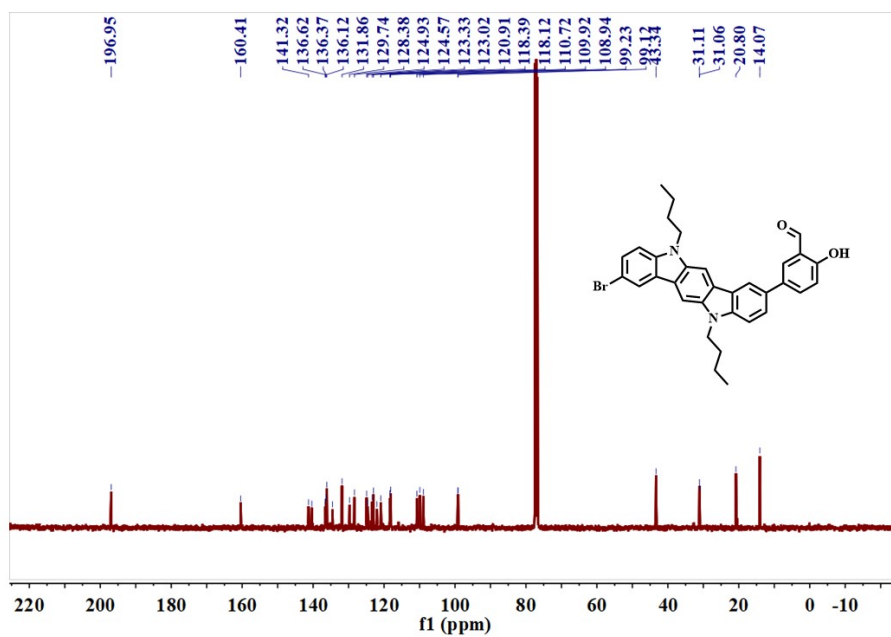
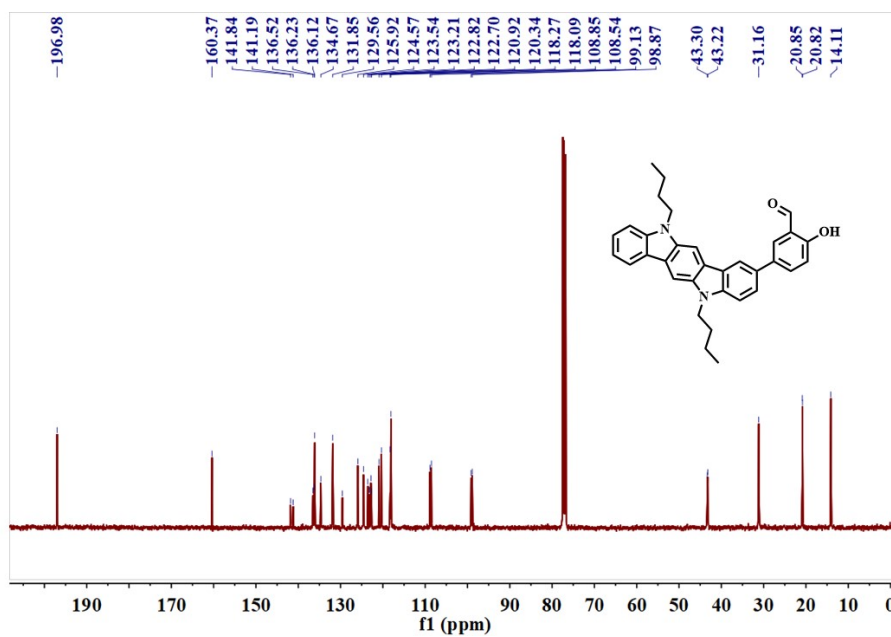


Fig. S2 ^{13}C NMR spectra of ICZ-p1-S and Br-ICZ-p1-S

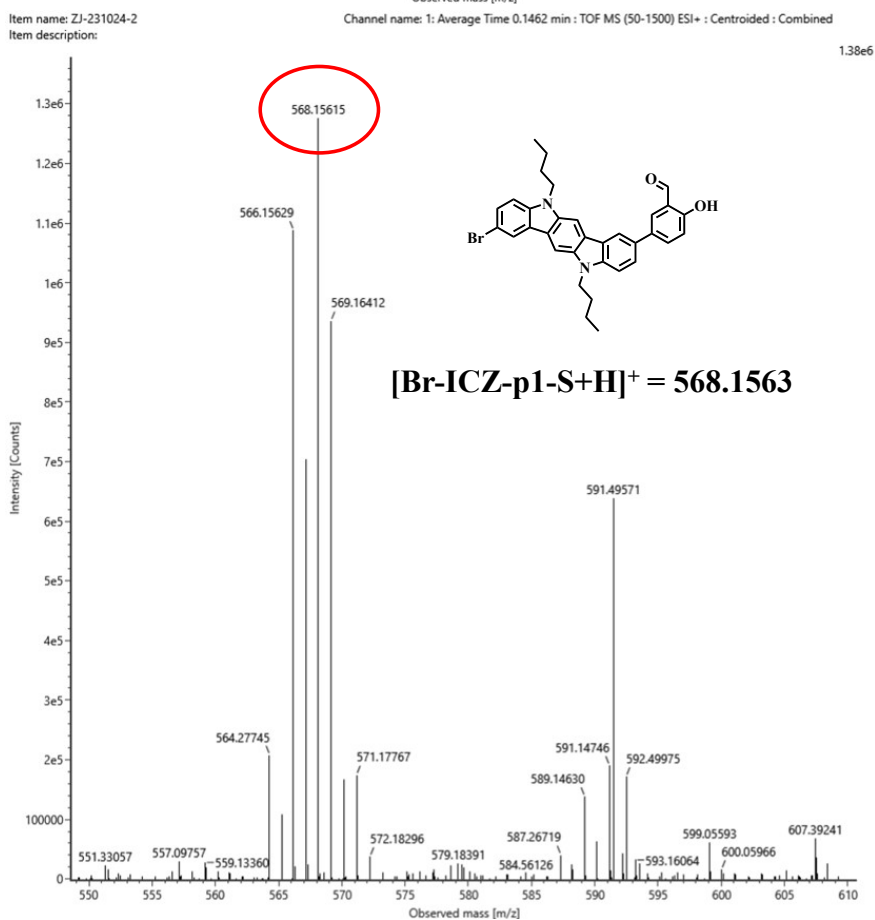
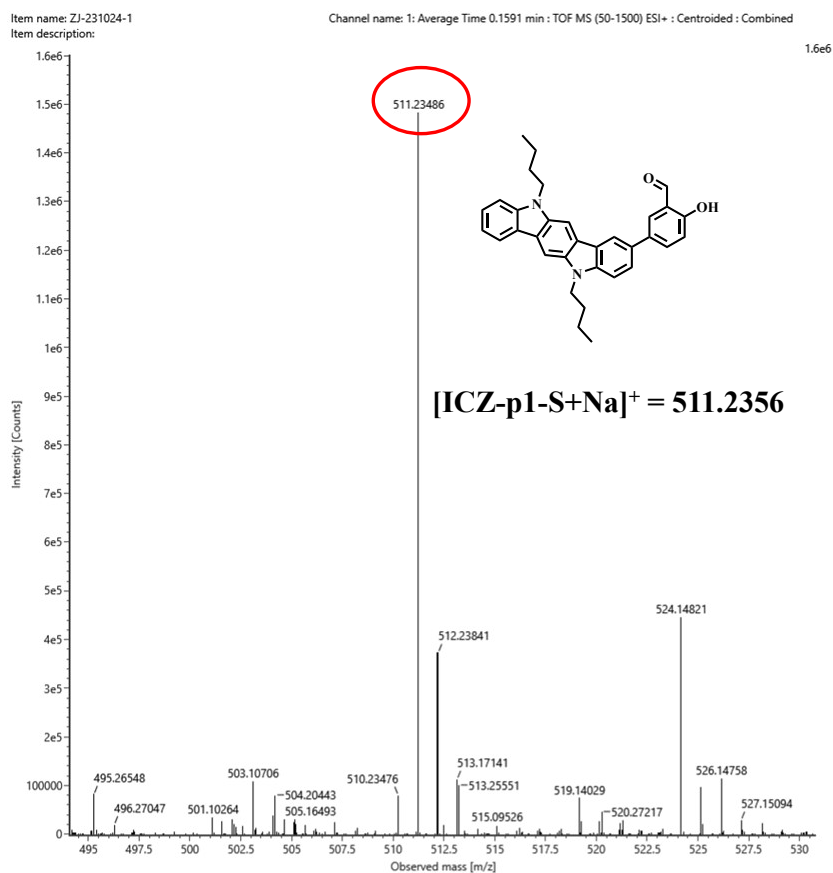


Fig. S3. High resolution mass spectra of ICZ-p1-S and Br-ICZ-p1-S

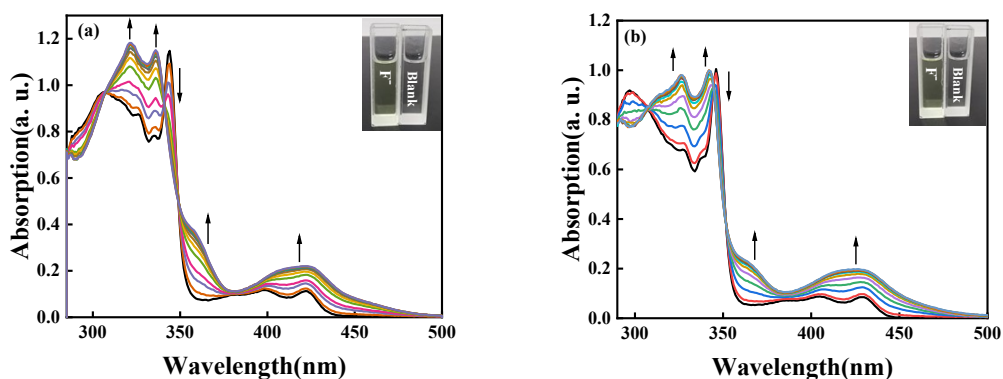


Fig. S4. UV-Vis spectra of the sensor interacting with different multiples of F^- : (a) ICZ-p1-S, (b) Br-ICZ-p1-S.

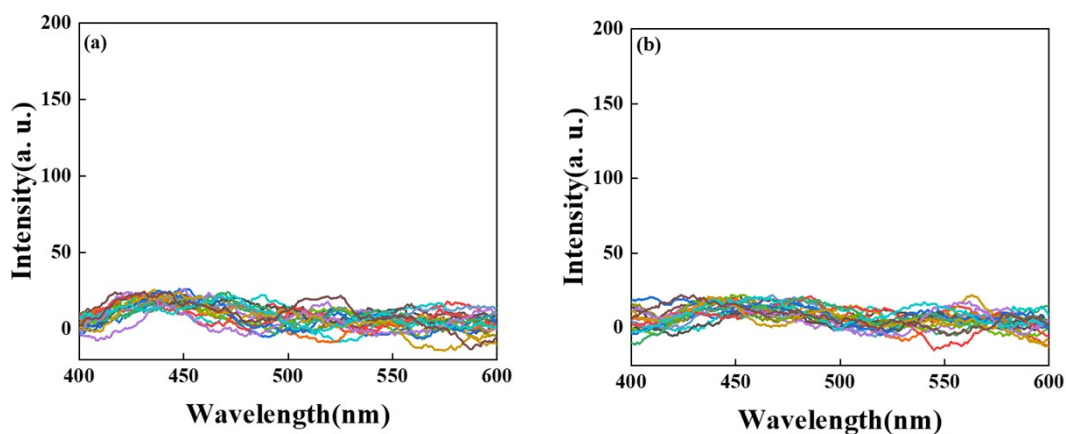


Fig. S5. Fluorescence spectra of the blank sensor solutions measured with 20 times: (a) ICZ-p1-S was 0.52, (b) Br-ICZ-p1-S was 0.31.

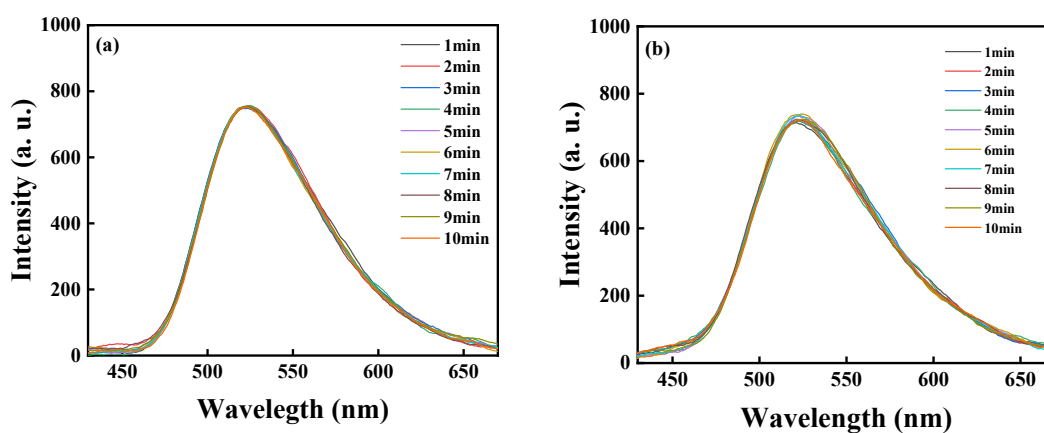


Fig. S6. Fluorescence spectra of sensor solutions with F^- at different times for the response time experiment.

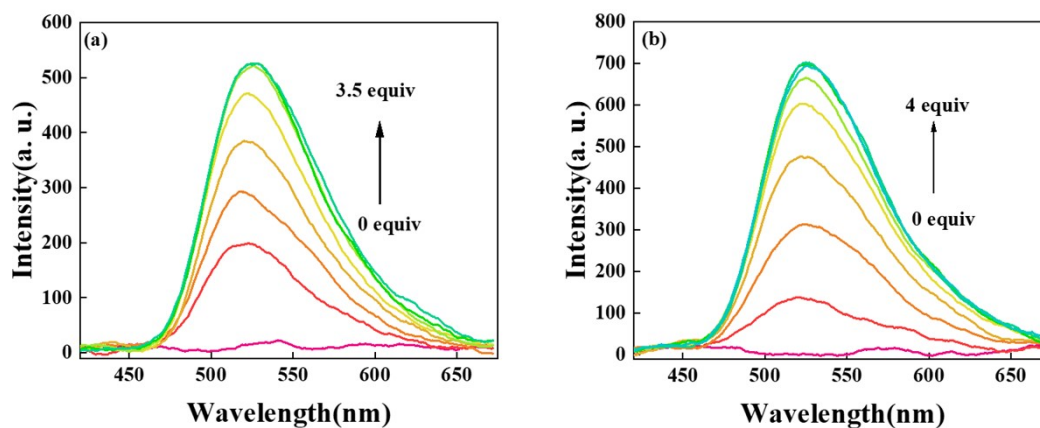


Fig. S7. Fluorescence spectra of sensor solutions with different multiples of F^- aqueous solutions: (a) ICZ-p1-S, (b) Br-ICZ-p1-S.

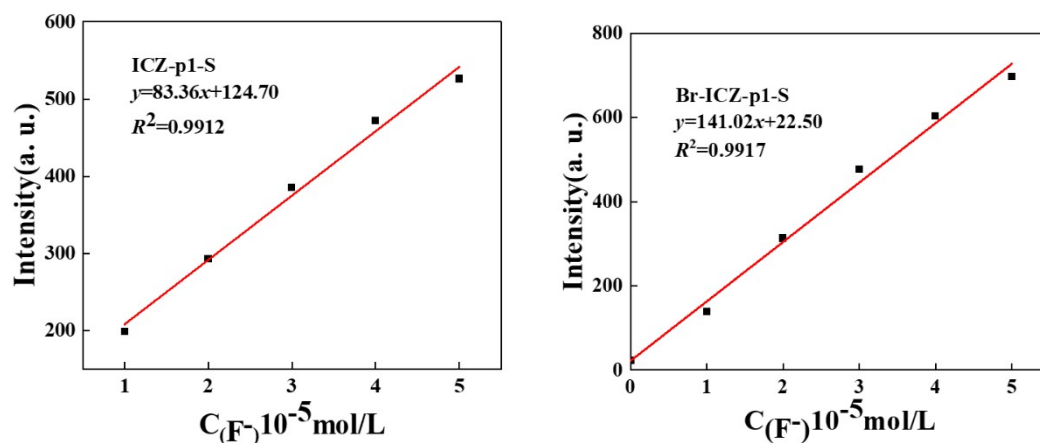
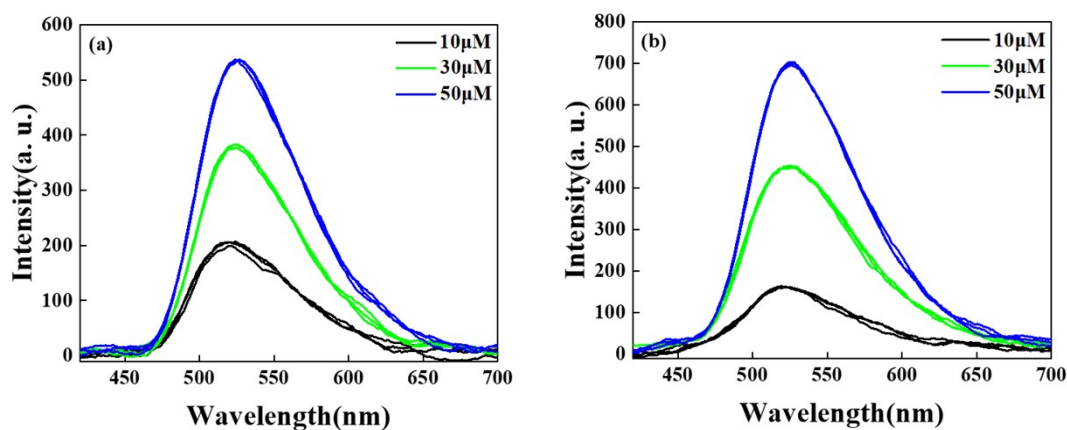


Fig. S8. Calibration curves of fluorescence intensities of sensors ICZ-p1-S and Br-ICZ-p1-S corresponding to aqueous solutions with different fluoride ion concentrations.



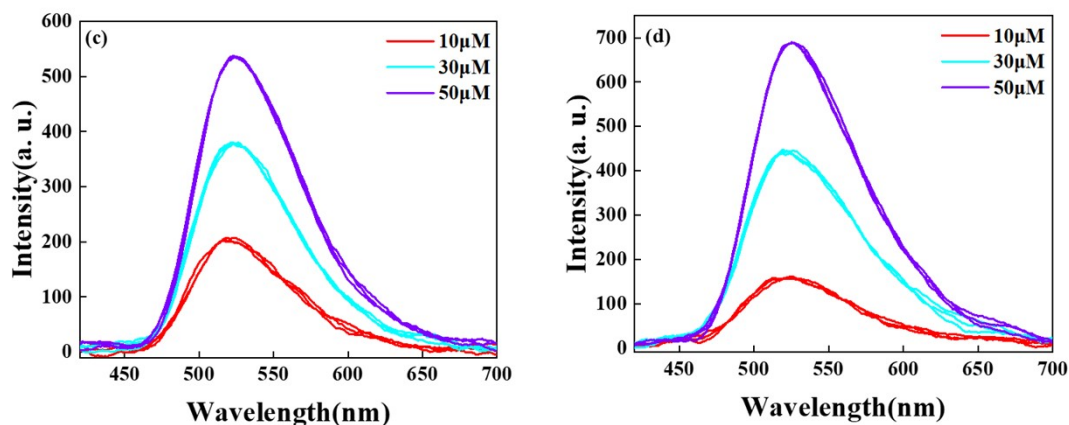


Fig. S9. Fluorescence intensities of solutions containing the sensors and tap water or Yuehu Lake water adding with 1 , 3 , and 5×10^{-5} mol/L fluoride ion solutions, respectively. Tap water: (a) **ICZ-p1-S**, (b) **Br-ICZ-p1-S**; Yuehu Lake water: (c) **ICZ-p1-S**, (d) **Br-ICZ-p1-S**.

Table S1. Single crystal data for **ICZ-p1-S**

Compounds	ICZ-p1-S
Empirical formula	$C_{33}H_{32}N_2O_2$
Molecular weight	488.63
Temperature (K)	298.15
Wavelength (\AA)	0.71073
Crystal system	monoclinic
Space group	P 21/n
a (\AA)	14.4740(12)
b (\AA)	12.9605(10)
c (\AA)	14.8707(12)
α ($^\circ$)	90
β ($^\circ$)	110.226(2)
γ ($^\circ$)	90
Volume (\AA^3)	2617.6(4)
Z	4
D_{calc} (g cm^{-3})	1.240
F (000)	1040.0
CCDC No.	2312194

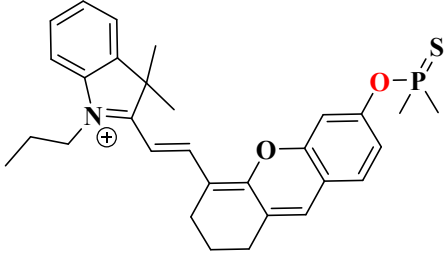
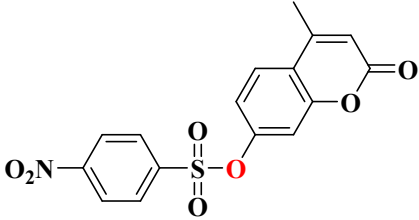
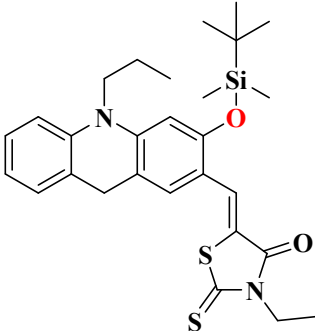
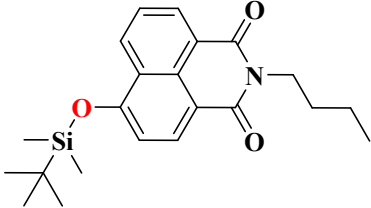
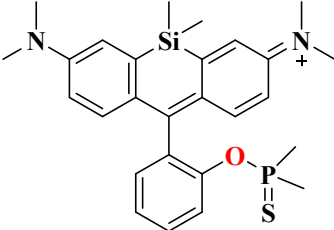
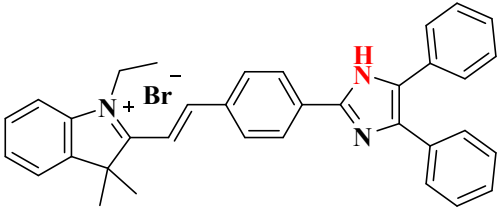
Table S2. Fluorescence intensities of solutions containing sensor and the real water samples spiked with different fluoride ion concentrations, as well as the determined actual fluoride ion concentration.

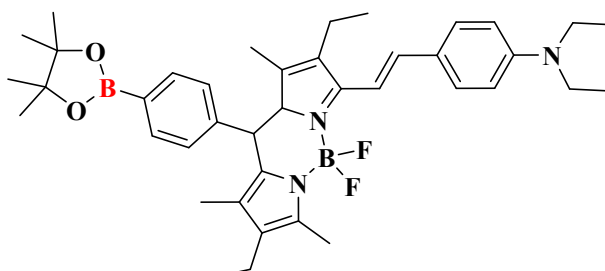
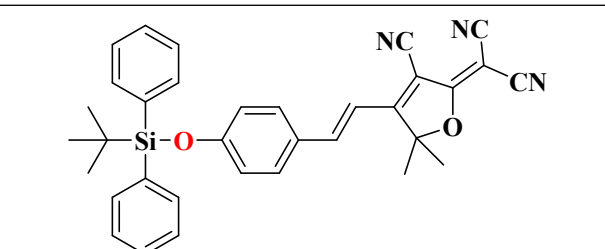
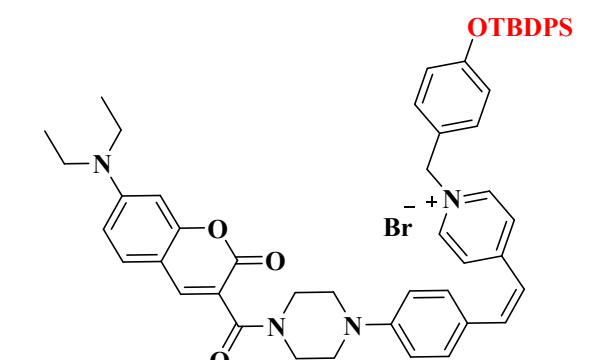
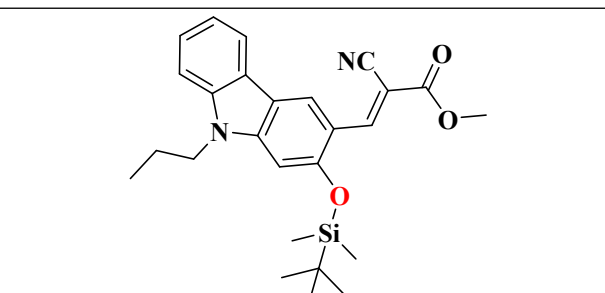
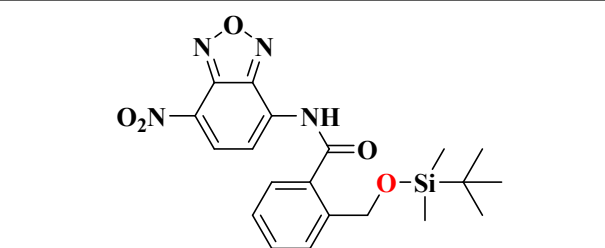
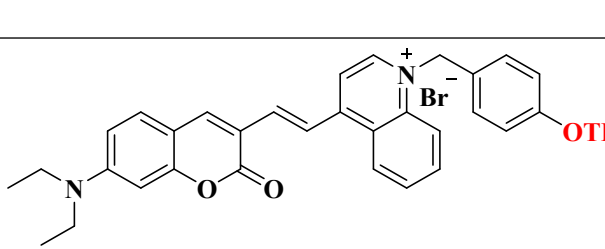
Sensor ICZ-p1-S									
Tap water									
$C_{\text{taken}} (10^{-5} \text{ M})$	1.00			3.00			5.00		
Intensity (a. u.)	207.05	206.16	199.12	383.09	383.27	377.40	537.22	537.00	534.42
$C_{\text{found}} (10^{-5} \text{ M})$	0.9879	0.9772	0.8928	3.0673	3.1018	3.0314	4.9887	4.9460	4.9151
River water									
$C_{\text{taken}} (10^{-5} \text{ M})$	1.00			3.00			5.00		
Intensity (a. u.)	206.96	202.61	201.26	378.39	377.36	379.92	534.49	535.46	537.48
$C_{\text{found}} (10^{-5} \text{ M})$	0.9868	0.9346	0.9184	3.0433	3.0310	3.0617	4.9159	4.9275	4.9518
Sensor Br-ICZ-p1-S									
Tap water									
$C_{\text{taken}} (10^{-5} \text{ M})$	1.00			3.00			5.00		
Intensity (a. u.)	162.96	163.54	161.40	453.59	451.80	453.04	703.33	700.47	695.18
$C_{\text{found}} (10^{-5} \text{ M})$	0.9960	1.0001	0.9850	3.0555	3.0442	3.0530	4.8279	4.8076	4.7701
River water									
$C_{\text{take}} (10^{-5} \text{ M})$	1.00			3.00			5.00		
Intensity (a. u.)	157.20	160.44	160.78	447.41	445.74	447.27	689.18	688.73	689.67
$C_{\text{found}} (10^{-5} \text{ M})$	0.9552	0.9782	0.9806	3.0131	3.0013	3.0121	4.7276	4.7244	4.7310

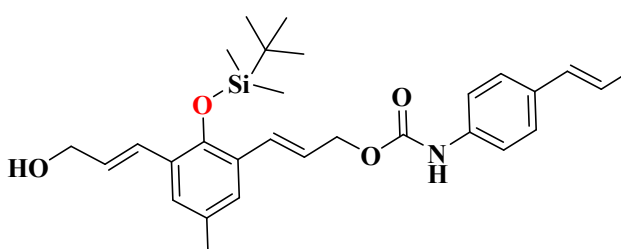
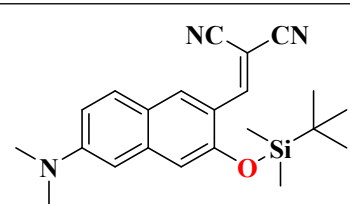
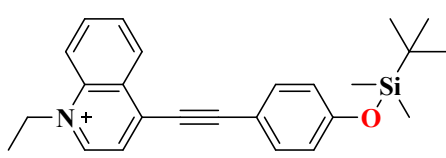
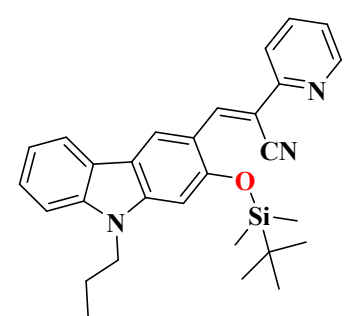
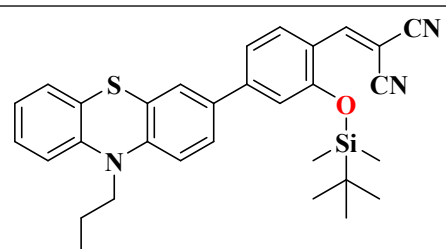
Table S3. Results of precision and accuracy using standard addition method for these sensors ($2.0 \times 10^{-5} \text{ M}$), three sets of parallel experiments ($n=3$) were determined. Tap water and Yuehu lake water from Guizhou University are used.

Sample	[Taken]/M	[Found]/M	R%	RE%	RSD%
Tap water	1.00×10^{-5}	$0.95 \times 10^{-5} / 0.99 \times 10^{-5}$	95.0/99.0	-4.74/-0.63	5.468/0.786
	3.00×10^{-5}	$3.07 \times 10^{-5} / 3.05 \times 10^{-5}$	102.3/101.7	2.23/1.70	1.147/0.195
	5.00×10^{-5}	$4.95 \times 10^{-5} / 4.80 \times 10^{-5}$	99.0/96.0	-1.00/-3.92	0.747/0.611
River water	1.00×10^{-5}	$0.95 \times 10^{-5} / 0.97 \times 10^{-5}$	95.0/97.0	-5.34/-2.87	3.78/1.443
	3.00×10^{-5}	$3.05 \times 10^{-5} / 3.01 \times 10^{-5}$	101.7/100.3	1.51/0.29	0.507/0.217
	5.00×10^{-5}	$4.93 \times 10^{-5} / 4.73 \times 10^{-5}$	98.6/94.6	-1.34/-5.45	0.371/0.070

Table S4. Some reported sensors with F⁻ response characteristics.

Sensor	Response time	Ref.
	10 s	Spectrochimica Acta Part A: Molecular and Biomolecular Spectroscopy, 2021, 252: 119518.
	1 min	Spectrochimica Acta Part A: Molecular and Biomolecular Spectroscopy, 2019, 211: 125-131.
	1 min	Dyes and Pigments, 2022, 201: 110200.
	3 min	Dyes and Pigments, 2011, 91(3): 442-445.
	6 min	Analytica Chimica Acta, 2018, 1030: 172-182.
	5-10 min	Spectrochimica Acta Part A: Molecular and Biomolecular Spectroscopy, 2018, 204: 777-

		782.
	10 min	ACS Omega 2022, 7 (38), 34317-34325
	25 min	Biosensors and Bioelectronics, 2014, 52: 298- 303.
	30 min	Spectrochimica Acta Part A: Molecular and Biomolecular Spectroscopy, 2024, 309: 123822.
	30 min	Chemical Papers, 2023, 77(3): 1741-1749.
	30 min	Tetrahedron letters, 2015, 56(35): 4975- 4979.
	30 min	
	35 min	Journal of Photochemistry and Photobiology A: Chemistry, 2020, 390:

		112349.
	40 min	Spectrochimica Acta Part A: Molecular and Biomolecular Spectroscopy, 2019, 220: 117108.
	60 min	Chemical Communications, 2012, 48(82): 10243-10245.
	90 min	Analytica chimica acta, 2005, 539(1-2): 311-316.
	150 min	Spectrochimica Acta Part A: Molecular and Biomolecular Spectroscopy, 2023, 285: 121816.
	240 min	Journal of Fluorescence, 2023: 1-9.

1. Ioele, M., et al., *A rapid and convenient synthesis of tetrakis (triphenylphosphine) palladium (O) and-platinum (O) complexes by phase-transfer catalysis*. 1991. **10**(20-21): p. 2475-2476.
2. Chen, Q., et al., *Improving anion sensing ability of the indolocarbazole-based fluorescence turn-on sensor by increasing salicylaldehyde response unit*. 2023. **265**: p. 124887.
3. Shi, H., et al., *Two novel indolo [3, 2-b] carbazole derivatives containing dimesitylboron moieties: Synthesis, photoluminescent and electroluminescent properties*. 2014. **38**(6): p. 2368-2378.

4. Shi, H.-p., et al., *Synthesis, photophysical and electrochemical properties and theoretical studies on three novel indolo [3, 2-b] carbazole derivatives containing benzothiazole units*. 2012. **68**(47): p. 9788-9794.